IRREVERSIBILITY IN THE GALTON BOARD VIA CONSERVATIVE CLASSICAL AND QUANTUM HAMILTONIAN AND GAUSSIAN DYNAMICS

William G. HOOVER

Department of Applied Science, University of California at Davis-Livermore and Center for Systems Far From Equilibrium, Lawrence Livermore National Laboratory, Livermore, CA 94550, USA

Bill MORAN

Earth Sciences Department, Lawrence Livermore National Laboratory, Livermore, CA 94550, USA

Carol G. HOOVER

National Magnetic Fusion Energy Computer Center and Center for Systems Far From Equilibrium, Lawrence Livermore National Laboratory, Livermore, CA 94550, USA

and

William J. EVANS

Department of Applied Science, Harvard University, Cambridge, MA 02138, USA

The periodic Galton board is analyzed from twin equivalent classical viewpoints: constrained gaussian isokinetic mechanics and unconstrained conservative hamiltonian mechanics. Both problems display chaotic fractal behavior. We also investigate the corresponding *quantum* Galton board using a novel numerical technique incorporating Gauss' principle of least constraint in the nonequilibrium Schrödinger equation.

1. Introduction

Chaotic motion is the fundamental mechanism underlying the second law of thermodynamics [1,2]. The exponentially-fast divergence, in some phase-space directions, of neighboring trajectories, coupled with the exponentially-even-faster trajectory convergence, in other directions, has two effects: the *divergence* guarantees sensitive dependence on initial conditions – future-information loss. The *convergence* guarantees the steady past-information loss which characterizes dissipative systems [3] but is also present in reversible equilibrium systems. Trajectory divergence [4,5] and convergence [6,7] in phase-space trajectories have by now been studied quantitatively for systems of several dozen particles,

both at and away from equilibrium [7]. The characteristic time scale of the phase-space deformations is the atomic collision time and the detailed "Lyapunov spectra" of these times has a simple power-law form reminiscent of the Debye distributions of solid-state physics. The Lyapunov spectrum has also a direct quantitative connection to the fractal phase-space dimensionality which characterizes steady nonequilibrium states [8].

The relationship between conservative and dissipative systems as well as the connection between classical and quantum chaos (if the latter exists [9]!) can only be understood fully for relatively simple models. We believe that the Galton board [10], or Lorentz gas [11,12] is, like Fermi's accelerator, the Nosé oscillator [13], the Hénon–Heiles problem

[14], and the Lorenz model of Rayleigh–Bénard instability [15], complex enough to reveal interesting physical behavior while remaining (numerically) tractable. The Galton board model also provides a novel link between dissipative and conservative mechanics.

In section 2 we describe the model and the three forms of mechanics (Gauss, Hamilton, and Schrödinger) used here to study its behavior. In section 3 we chronicle briefly the development of our numerical solution method for the quantum problem, and describe the simplest prototypical sample of the results obtained so far.

Our work on the quantum problem is exploratory and suggests many related applications. We particularly wish to urge the investigation of both the model and the gaussian constraint technique by others in order to elucidate further the connection between classical and quantum chaos (if the latter exists!).

2. Galton board mechanics

The Galton board is often used to illustrate the binomial distribution [10]. A particle dropped into the top of a triangular-lattice array of scatterers, and proceeding either to the right or to the left as it falls, generates, on the average, the binomial distribution at the bottom of the board. By replacing the linear-potential gravitational field with an electric field the same idea can be used to caricature electronic solid-state diffusion. Fig. 1 illustrates the trajectory of a single scattering particle proceeding through the board, under the influence of an external field, making elastic collisions with perfectly hard (two-dimensional) disks. The board dynamics can be used to generate an equivalent dynamics for a two-body periodic system by switching to a coordinate system fixed on one of the two bodies [11].

It might appear that one could determine a conductivity for the board, viewed as a problem in conservative hamiltonian mechanics, by measuring the mean velocity as a function of field strength. But the problem is not that simple. The increase in kinetic energy K, as the particle falls in the linear potential $\Phi = -Ex$, with a constant-field linear-potential hamiltonian,
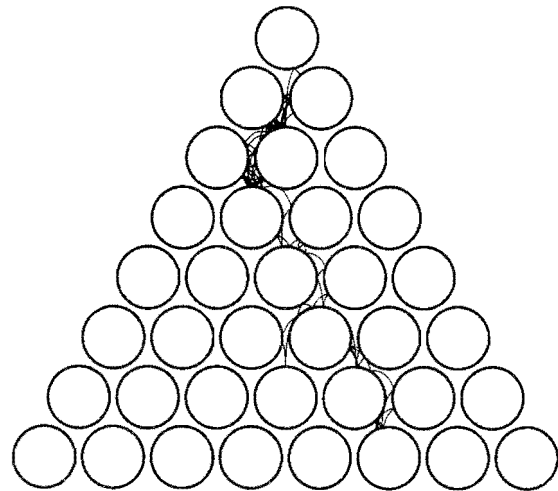
Fig. 1. A Galton board trajectory showing a series of 99 collisions. As explained in the text, the trajectories shown here for a constant field, $E = 4p^2/m\sigma$, using isokinetic mechanics, are identical to those using an exponentially-increasing field and hamiltonian mechanics.

$$H_{\text{linear}} = K + \Phi = p^2/2m - Ex, \qquad (1)$$

leads to large current fluctuations, making it difficult to obtain an estimate of the conductivity. This problem of inhomogeneous fluctuations can be overcome by considering an ensemble of falling particles, but the resulting average still does not describe a steady state. An accurate ensemble estimate for the linear conductivity is available from the indirect approach of Green–Kubo linear-response theory [12].

In the conservative hamiltonian case just discussed, with a constant field E, the influence of the field on the particle trajectories decreases, due to the increase of kinetic energy with penetration into the board. There is therefore no nonequilibrium steady state. An alternative approach, which *does* lead to a nonequilibrium steady state, is to use constrained gaussian mechanics [16]. To do so we can artificially constrain the falling particle to fall at a constant speed. This can be done in many ways [17]. We chose to follow Gauss, using his principle of least constraint [16,18], which used the *minimum* ("least") possible constraint force necessary. The constrained trajectories are more complicated than the hamiltonian parabolas. Between collisions they have the form

$$\Delta x = (p^2/mE)\ln(\sin\theta_0/\sin\theta), \qquad (2a)$$

$$\Delta y = (p^2/mE)(\theta_0 - \theta), \qquad (2b)$$

$$t = (p/E)\ln[\tan(\theta_0/2)/\tan(\theta/2)], \qquad (2c)$$

where the variable θ describes the direction of motion relative to the field direction. The velocity vector has a fixed magnitude p/m. A sample 99-collision Galton board trajectory, using these gaussian equations of motion in a relatively strong field, is shown in fig. 1.

The declining influence of the field E can alternatively be overcome by making the field stronger as the particle falls. As simple dimensional analysis would suggest, choosing a *nonlinear* potential which maintains a constant ratio between the kinetic and potential energies guarantees that the curvature of the trajectories due to the field is independent of x. To simplify the argument, suppose that the (conserved) value of the hamiltonian is zero. Then the particle velocity, by conservation of energy, varies as $(-\Phi/m)^{1/2}$. The time between collisions varies as the inverse of the speed, $\tau_c \sim \sigma(-\Phi/m)^{-1/2}$, so that the deflection induced by the field $-d\Phi/dx$, varies as $(-d\Phi/dx)/\Phi$. Thus, the depth of penetration into the board does not affect the shape of the trajectories provided that a nonlinear exponential-potential hamiltonian is used:

$$H_{\text{nonlinear}} = K - E\lambda e^{x/\lambda}, \qquad (3)$$

where the characteristic length λ is a parameter describing the nonlinearity of the field. The dimensionless ratio of the scatterer diameter σ to the length λ characterizes the departure of the nonlinear from the linear problem.

The equations of motion, between the elastic hard-disk collisions, can be solved analytically for the constrained gaussian dynamics (constant field) or for unconstrained hamiltonian dynamics (exponentially increasing field). It is astonishing that the two very different functional forms lead to identical trajectories, as described by the first two of eqs. (2) above. That is the parametric dependence of the x and y deflections on the direction of motion θ, are given by (2a) and (2b) in both cases, provided that the nonlinear scale length λ is related to the linear field strength E by the relation

$$\lambda E = p^2/2m. \qquad (4)$$

It is by no means obvious, but is true, that the trajectories are identical; that is, the xy tracks of the scattering particles are identical in the constant-field and exponentially-increasing-field cases.

The time behavior is very different in these two cases. In the constant-field isokinetic case the moving mass-point particle obviously requires an infinite time to travel infinitely far. In the exponentially-increasing-field hamiltonian case the moving particle instead arrives at infinity after a *finite* amount of time. (This perhaps surprising result can be seen easily by considering that the times to penetrate a series of fixed lengths form a geometric series, and hence sum to a finite rather than infinite total time.)

The divergence of velocity just described might suggest an examination of the *relativistic* Galton board, but action-at-a-distance in relativity theory is traditionally viewed with distaste. Authors such as Pars [18] describe the dynamics of "particles with variable mass" partly in order to circumvent the action-at-a-distance paradox. There is no problem in viewing the motion of a mass point at high speeds, but the hard-disk interaction resists Lorentz contraction and is therefore paradoxical. If one persists in developing the extreme relativistic equations, these reduce also to the same form as those derived from the nonlinear-potential hamiltonian, $H_{\text{nonlinear}}$, but with the speed replaced by its maximum value c.

We previously pointed out that by incorporating the (nonholonomic) constraint of fixed kinetic energy K the board could be forced to yield a finite, well-defined conductivity [11] consistent with the Green-Kubo calculations of Machta and Zwanzig [12]. The corresponding trajectory calculations revealed an interesting fractal phase-space structure, which has since been characterized for a variety of nonequilibrium systems and used to resolve Loschmidt's paradox [1]. See figs. 2 and 3 for two different views of this structure. But the equivalence of these fractal trajectories with the hamiltonian nonlinear-field trajectories suggests yet another paradox: How can fractal trajectories describe also the dynamics of a conservative hamiltonian system obeying Liouville's theorem with a constant phase-space volume? This equivalence paradox can be resolved by noting that the convergence of trajectories in the phase-space
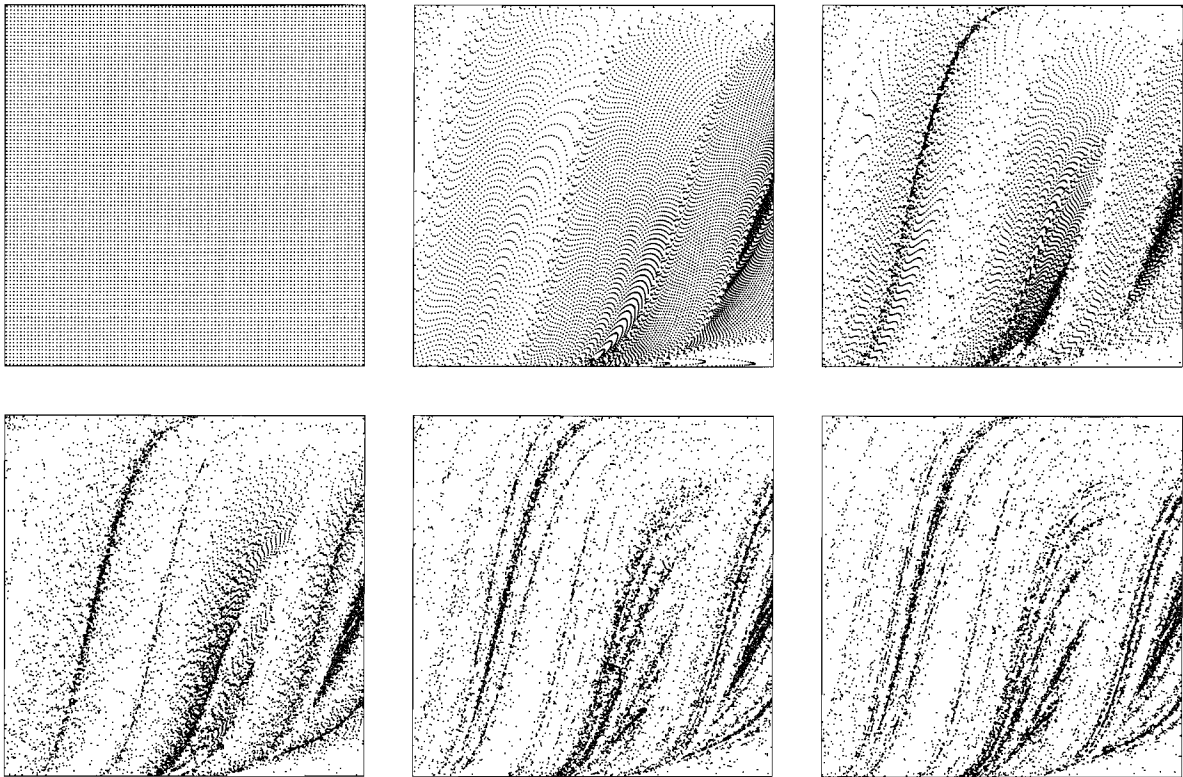
Fig. 2. Time development of 10 000 Galton board trajectories for a field $E = 3p^2/m\sigma$ indicating the convergence of phase-space volume to a strange attractor. The ordinate is the sine of the angle, relative to the normal, made by the velocity after collision. The abscissa is the angle at which the collision occurs relative to the field direction. Thus a head-on collision at the "top" of a scatterer corresponds to a point at the middle of the right-hand boundary of these phase-space sections. The Poincaré-section views shown correspond to 10 000 phase-space states occupied after 0, 1, 2, 3, 5, and 10 collisions.

plane of the Poincaré section characterizing collisions (shown in fig. 2) is exactly offset by *divergence* normal to that plane as the velocity approaches infinity.

Thus the *same* trajectories can be described with either dissipative gaussian or conservative hamiltonian dynamics, either relativistic or nonrelativistic. The relationship between the trajectories can be further elucidated by time scaling, as discussed in Nosé's closely-related extension of hamiltonian mechanics to gibbsian statistical mechanics [19,20]. If the time scales according to the local velocity, such that

$$(p/m) \, \mathrm{d}t_{\text{scaled}} = (p_0/m) \, \mathrm{d}t_{\text{unscaled}}, \qquad (5)$$

then the linear, nonlinear, and extreme-relativistic trajectories all coincide.

Ford [9] has emphasized, tenaciously and elo-

quently, that the validity of quantum mechanics may be linked with its ability (or inability) to describe the chaos that is pervasive in classical physics. For this reason the quantum Galton board deserves study. Because our initial efforts were frustrating and time-consuming, despite the inspiration of much seminal work on numerical quantum mechanics in the literature, we outline the quantum development here, in the following section.

3. Schrödinger–Gauss Galton board dynamics

Heller [21] and several others have pioneered calculations of high-energy quantum states for classically-chaotic stadium problems, and the form of the spectrum for such models has also been carefully in-
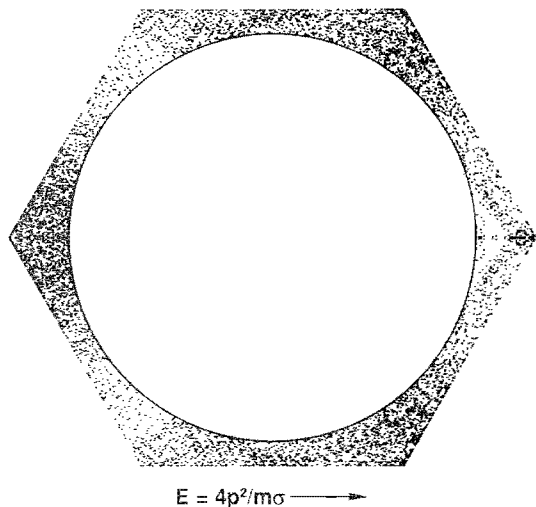
$$E = 4p^2/m\sigma \longrightarrow$$

Fig. 3. Time-averaged configurational probability density for a 300-collision segment of a classical Galton board trajectory with a field $E=4p^2/m\sigma$. The density function has been symmetrized relative to the horizontal bisector of the hexagonal cell.

Table 1
Scatterer sizes well-suited to a hexagonal triangular-lattice grid. Each scatterer type listed below excludes n sites lying within a radius r of a triangular-lattice origin site, and including 48 sites at exactly the distance r indicated in the table. The first entry in the table, for instance, includes the (x, y) pairs $(41.5, 5\sqrt{3})$, $(41.0, 4.0\sqrt{3})$, $(39.5, 7.5\sqrt{3})$, and $(36.5, 11.5\sqrt{3})$ lying between 0 and 30°. The other 44 sites at a radius of $\sqrt{1729}$ follow from symmetry. The excluded area, $\sqrt{3}/4$ per excluded site, is also compared to the area of an equivalent circle.

r^2	Sites	Area/πr^2
1729	6283	1.00173
2821	10279	1.00445
3367	12223	1.00073
3913	14233	1.00269
4123	14995	1.00257

vestigated. For finite potentials, such as the Hénon–Heiles model, Feit and Fleck [14] have instead used fast-Fourier-transform methods to follow a solution of the time-dependent Schrödinger equation

$$i\partial\psi/\partial t = -\tfrac{1}{2}\nabla^2\psi + \Phi\psi, \qquad (6)$$

where the potential energy Φ describes the field. We follow tradition in setting $h/2\pi$ and m equal to unity in the quantum problem. In Heller's simply-connected stadium problems, which resemble the Galton board without the complexity of the periodic boundaries, the potential term is missing and a Fourier representation of ψ can be found which satisfies the boundary conditions at many "collocation points". For continuous potentials the kinetic energy can conveniently be worked out in Fourier space (where multiplying by k^2 is equivalent to operating with $-\nabla^2$) and the potential can be Fourier analyzed in real space. Both methods result in highly-accurate wave functions and energy eigenvalues.

Here we are interested primarily in studying the behavior of the nonlinear quantum problem in which a nonequilibrium steady state is imposed. We began by applying Heller's boundary-collocation technique at selected points around the boundary of a single nearly-circular elastic scattering disk confined to a periodic unit cell. Table 1 describes scatterer choices which are specially well-suited to a hexagonal grid. But superpositions of isokinetic plane waves, chosen either equally-spaced or at random always yielded a poorly-behaved function in between the fitting points. Additional constraints on the wave function first derivative at the collocation points did not improve the situation.

We abandoned the Fourier technique altogether and instead formulated the problem as a finite-difference problem on a triangular-lattice grid. In this approach the spatial derivatives are approximated as finite differences while the time variation is treated accurately. We arbitrarily choose a nearest-neighbor grid spacing of unity. It is now (1988) feasible to use grids with up to about 10^5 grid points. Thus, the laplacian operator ∇^2 is evaluated by summing two-thirds the (six) nearest-neighbor wave-function values and subtracting four times the local value. Similarly wave-function gradients are approximated by taking first differences of nearest-neighbor wave-function values. In this way the Schrödinger equation (6) becomes a set of $2N$ linear ordinary first-order differential equations for the N nonvanishing real and imaginary wave-function values. The wave function is extended across the periodic boundary in the usual way and is set equal to zero inside the scatters. *This idea has the advantage that mass and energy are conserved exactly.*

The solution is a linear combination of N eigenfunctions periodic in space and time. These are the "normal-mode" solutions of $\partial^2\psi/\partial t^2 = -\tfrac{1}{4}\nabla^4\psi$. But

it is more convenient to follow the time-dependence numerically. The integration of the ordinary differential equations, using the classic fourth-order Runge–Kutta method with a timestep of order 0.1, typically conserves both the mass (summed value of $\psi^2 = \psi^{r2} + \psi^{i2}$) and the kinetic energy (summed value of $-\frac{1}{2}(\psi^r \nabla^2 \psi^r + \psi^i \nabla^2 \psi^i)$) to seven significant figures.

Although the nonlinear-field case can be treated in this way the assignment of phase across the boundaries is a nontrivial problem. On the other hand the wavefunction amplitude can be easily estimated semiclassically. That is, for a steady state the mass flux integrated normal to the field direction must be constant. Because the probability of observation varies as the inverse of the classical speed, which in turn varies as the square root of the kinetic energy, the wave function amplitude $(\psi^2)^{1/2}$ varies as the fourth root of the kinetic energy, that is $\psi_{\text{nonlinear}}$ varies as $\exp(-x/4\lambda)$, where x is the coordinate in the direction of increasing field.

But a constrained solution of the Schrödinger equation with a fixed current yields a geometrically-simpler, but mathematically-more-complicated solution than that obtained with a nonlinear field. To solve this constrained problem, we use Gauss' principle of least constraint to impose the requirements that mass, momentum, and energy be constants of the motion. (The quantum values correspond to averages over a classical ensemble.) These conditions are

$$C_1 = \sum \tfrac{1}{2}(\psi^r\psi^r + \psi^i\psi^i) - \tfrac{1}{2}N = 0,$$
$$C_2 = \sum (\psi^r \nabla \psi^i - \psi^i \nabla \psi^r) - NI = 0,$$
$$C_3 = \sum -\tfrac{1}{2}(\psi^r \nabla^2 \psi^r + \psi^i \nabla^2 \psi^i) - N\epsilon = 0. \qquad (7)$$

In (7) N is the number of available sites – that is, sites lying outside the excluded area of the periodic scatterer. I is the current and ϵ is the energy per occupied site. Because we use a discrete mesh of sites both these quantities have a finite range of values. Using the finite-difference form of the constraints (7) replaces each constraint by a quadratic form in the $\{\psi^r\}$ and $\{\psi^i\}$. The Schrödinger equation of motion does not generally conserve momentum, because scattering occurs at the sites where ψ^r and ψ^i vanish. Instead the unconstrained momentum sum tends to oscillate, with a period of a few dozen timesteps. Gauss' principle of least constraint can be extended to the quantum case by requiring that the wavefunction be changed as little as possible in order to satisfy the constraints C_1, C_2, and C_3. All three constraints can be satisfied simultaneously by adding three Lagrange multipliers to the equation of motion:

$$(\partial\psi/\partial t)_{\text{Gauss}} = (\partial\psi/\partial t)_{\text{Schrödinger}}$$
$$- \alpha\nabla C_1 - \beta\nabla C_2 - \gamma\nabla C_3. \qquad (8)$$

This analog of Gauss' principle of least constraint could similarly be extended to parallel Nosé's extension of hamiltonian mechanics. Each gradient in (8) is computed with respect to the corresponding wavefunction amplitude appearing on the left-hand side. Because the multipliers α, β, and γ depend upon ψ the resulting equation is *nonlinear*. Just as in the classical case the equation of motion (8) is time-reversal-invariant. Going *backward* in time ψ^r, α, and γ are unchanged while ψ^i and β change sign. The Lagrange multipliers have an obvious thermodynamic significance, with β playing the role of an external work-performing force and γ playing the role of a compensating heat-extracting thermostat. Numerical tests have shown that the constrained quantum solutions are well-behaved and do correspond to nonequilibrium steady quantum states which are directly comparable to the classical Galton board solutions discussed in the first two sections.

The quotient, $\langle d\epsilon/dt \rangle / I^2$, is a phenomenological conductivity. We have related the current defined in eq. (7) to such a phenomenological transport theory in two ways. We first *estimated* the rate at which energy would increase using Schrödinger mechanics (6) if the energy-constraining Lagrange multiplier γ in the Gauss dynamics (8) were to be instantaneously set equal to zero. Next we studied gaussian systems with constrained mass and momentum, but with the energy free to increase or decrease. This gave a second estimate for $\langle d\epsilon/dt \rangle$ as a function of I. Both approaches yielded consistent results for the conductivity. The second approach is limited to short times because the energy for a finite grid is bounded.

Our preliminary investigation was carried out for a simple system containing $5 \times 5 = 25$ sites, with the central 7 sites excluded by a single periodically-repeated scatterer. We solved the set of the 36 coupled nonlinear ordinary differential equations for ψ^r and

ψ^i, with N fixed at 18, I fixed at 0.1, 0.2, or 0.5, and an initial energy, $N\epsilon$, of 15. The corresponding conductivities, 1.6, 1.2, and 0.9, show an effective field dependence similar to the classical results discussed in ref. [11].

These numerical results are gratifying. At the same time, *movies* of the wavefunctions show very clearly and convincingly the moving waves associated with such a nonvanishing current. Time averages of the quantum probability and current can be expected to resemble their classical-mechanical, elastic, and hydrodynamic analogs. We expect to carry out a detailed investigation of the quantum–chaos correspondence limit in the near future.

Acknowledgement

References

[1] B.L. Holian, W.G. Hoover and H.A. Posch, Phys. Rev. Lett. 59 (1987) 10.

[2] H.A. Posch and W.G. Hoover, Phys. Rev. A 38 (1988) 473.

[3] R. Shaw, Z. Naturforsch. A 36 (1981) 80.

[4] S.D. Stoddard and J. Ford, Phys. Rev. A 8 (1973) 1504.

[5] G. Benettin, L. Galgani and J.M. Strelcyn, Phys. Rev. A 14 (1976) 2338.

[6] W.G. Hoover and H.A. Posch, Phys. Lett. A 113 (1985) 82; 123 (1987) 227;
G.P. Morriss, Phys. Rev. A 37 (1988) 2118.

[7] H.A. Posch and W.G. Hoover, Equilibrium and nonequilibrium Lyapunov spectra for dense fluids and solids, Phys. Rev. A, submitted, August 1988.

[8] J. Kaplan and J. Yorke, in: Lecture notes in mathematics, Vol. 730. Functional differential equations and the approximation of fixed points, eds. H.O. Peitgen and H.O. Walther (Springer, Berlin, 1980).

[9] J. Ford, Directions in classical chaos, in: Directions in chaos, Vol. 1, ed. H. Bai-Lin (World Scientific, Singapore, 1988) p. 1.

[10] M. Kac, Sci. Am. 211(9) (1964) 92.

[11] B. Moran, W.G. Hoover and S. Bestiale, J. Stat. Phys. 48 (1987) 709.

[12] J. Machta and R.W. Zwanzig, Phys. Rev. Lett. 50 (1983) 1959.

[13] H.A. Posch, W.G. Hoover and F.J. Vesely, Phys. Rev. A 33 (1986) 4253.

[14] M.D. Feit, J.A. Fleck Jr. and A. Steiger, J. Comp. Phys. 47 (1982) 412;
M.D. Feit and J.A. Fleck Jr., J. Chem. Phys. 80 (1984) 2578.

[15] W.G. Hoover, C.G. Tull and H.A. Posch, Phys. Lett. A 131 (1988) 211.

[16] D.J. Evans, W.G. Hoover, B.H. Failor, B. Moran and A.J.C. Ladd, Phys. Rev. A 28 (1983) 1016.

[17] W.G. Hoover, Physica A 118 (1983) 111.

[18] L.A. Pars, A treatise on analytical dynamics (Oxbow Press, Woodbridge, CT, 1979).

[19] S. Nosé, Mol. Phys. 52 (1984) 255; J. Chem. Phys. 81 (1984) 511.

[20] S. Nosé, Mol. Phys. 57 (1986) 187.

[21] E.J. Heller, Qualitative properties of eigenfunctions of classically chaotic hamiltonian systems, in: Lecture notes in physics, Vol. 263. Quantum chaos and statistical nuclear physics, eds. T.H. Seligman and H. Nishioka (Springer, Berlin, 1986);
E.J. Heller and P.W. O'Connor, Nucl. Phys. B 2 (1987) 201;
M.V. Berry, Ann. Phys. 131 (1981) 163; Proc. R. Soc. A 413 (1987) 183.